PCCP

A discharge-flow study of Cl_2O_3

T. J. Green, M. Islam,† P. Guest, K. Hickson, C. E. Canosa-Mas and R. P. Wayne*

Physical and Theoretical Chemistry Laboratory, South Parks Road, Oxford, UK OX1 3QZ. E-mail: wayne@physchem.ox.ac.uk

Received 9th September 2003, Accepted 15th October 2003
First published as an Advance Article on the web 6th November 2003

The discharge-flow technique coupled with UV-absorption spectroscopy has been used to study the production of dichlorine trioxide, Cl_2O_3, from the reaction between ClO and OClO radicals. The absorption cross section of Cl_2O_3 was determined to be $(1.44 \pm 0.10) \times 10^{-17}$ cm^2 molecule^{-1} at $\lambda_{max} = 267$ nm (all errors reported are two standard deviations of the statistical error). The equilibrium constant for the process

$$ClO + OClO + M \rightleftharpoons Cl_2O_3 + M$$

was measured in the temperature range 243–298 K. A Second-Law analysis yielded values of $\Delta_r H^{\ominus} = -57.9 \pm 2.1$ kJ mol^{-1} and $\Delta_r S^{\ominus} = -132.6 \pm 7.9$ J K^{-1} mol^{-1}. The rate coefficient for the formation of Cl_2O_3 was measured with helium as the third body at a concentration of $\sim 7.3 \pm 10^{16}$ molecule cm^{-3} over the temperature range 243–283 K. Analysis of these data employing the conventional form of the rate equation for the low-pressure limit, $k^0(T) = k^0(300) \cdot (T/300)^{-n}$, resulted in values of $k^0(300) = (2.83 \pm 0.04) \times 10^{-32}$ cm^6 molecule^{-2} s^{-1} and $n = -4.32 \pm 0.1$. These spectroscopic, thermochemical and kinetic data are compared with previously reported values.

Introduction

Chlorine oxides have been extensively studied in the laboratory, particularly since they became implicated in stratospheric ozone loss, yet, although they have been investigated for roughly two centuries, our understanding of their complex chemistry is not yet complete. The chemical instability of chlorine oxides was noted as early as 1823, when Michael Faraday observed a violent explosion while attempting to prepare chlorine dioxide.[1] Chlorine dioxide, OClO, is a widely used precursor in many of the syntheses of the higher chlorine oxides. Photolysis of OClO has been reported as producing numerous other chlorine oxides, Cl_2O_7, Cl_2O_4, Cl_2O_3 and $ClClO_2$, depending on the experimental conditions chosen.[2]

The development of spectroscopy has been fundamental to expanding understanding of the complex chemistry of the chlorine oxides. Most of the oxides of chlorine absorb electromagnetic radiation in the region 200–450 nm, which makes them amenable to study by UV spectroscopy. However, there is considerable danger that overlapping absorptions may occur in a chemical system containing chlorine oxides, thus making the extraction of unique spectra difficult. Such difficulties are probably responsible for the widely differing relative intensities reported for many chlorine oxide spectra. While the concurrent use of IR- and UV-spectroscopy has aided unequivocal identification of chlorine oxides, the difficulty of obtaining uncontaminated samples, and the variety of different conditions under which measurements have been made, still complicate the studies.[3,4] Some workers have thus gone to great lengths to constrain the chemical system under study to avoid the contribution of unknown or mixed absorptions (see, for example, refs. 5 and 6).

Insight into chlorine oxide chemistry was provided from laboratory studies conducted after it was found that catalytic ozone depletion by a chain involving the *sym*-ClO dimer[7] is at least partially responsible for the appearance of ozone 'holes' in polar regions during springtime. The existence of O_3, OClO, ClO and Cl_2 in the polar stratosphere seemed to allow the possibility of complex atmospheric photochemistry in which the higher oxides of chlorine such as Cl_2O_3 might participate. Our improved understanding of stratospheric chemistry now indicates that these higher oxides of chlorine are unlikely to have a significant atmospheric role, with the exception of the ClO-dimer.[2] However, there are aspects of the chemistry of Cl_2O_3 that warrant further investigation, regardless of the participation of this oxide in atmospheric processes.

Cl_2O_3 was first detected by Lipscomb *et al.*[8] These workers subjected OClO to flash photolysis and detected Cl_2O_3 by UV absorption using photographic recording of the spectrum. Hayman and Cox[9] also studied the flash photolysis of OClO, Cl_2O_3 in this case being detected by UV absorption using a diode-array spectrometer. Hayman and Cox obtained data on the UV spectrum, equilibrium constants and kinetics of formation for a range of temperatures. Parr *et al.*[10] used the molecular-modulation technique to study the rate of formation of Cl_2O_3, while Burkholder *et al.*[11] used the flash-photolysis technique to obtain a large body of data on Cl_2O_3. Harwood *et al.*[12] subsequently studied Cl_2O_3 by the flash-photolysis technique coupled with UV absorption detection with a CCD spectrometer.

The most recent data compilation from NASA/JPL[13] makes it clear that there remain uncertainties about the quantitative spectroscopy of Cl_2O_3. Absorption cross sections for Cl_2O_3 have been presented by Hayman and Cox,[9] Burkholder *et al.*,[11] and Harwood *et al.*[12] that are consistent in broad outline, but that differ significantly in the spectral regions below $\lambda = 240$ nm and in the long-wavelength tail beyond $\lambda = 300$ nm. The reviewers[13] draw attention to the need for further research, especially with respect to the longer wavelength region.

All the previous studies have used the flash-photolysis technique to produce Cl_2O_3. Our aim was to study Cl_2O_3 by

† Current address: School of Science and Technology, University of Teesside, Middlesbrough, UK TS1 3BA.

a different technique, namely that of discharge-flow coupled with UV absorption using a diode-array spectrometer. This study is intended to complement, and in some respects extend, the previous flash-photolysis investigations.

Experimental

The use of a diode array spectrometer (DAS) allowed the 'multiplex' detection of spectra over an extended wavelength range. Most of the oxides of chlorine absorb electromagnetic radiation in the region 200–450 nm, which thus makes them amenable to study by UV spectroscopy. If overlapping of absorption features occurs, multichannel detection is essential to deconvolute the spectra of any broad band absorbers. The structured regions of the $A\,^2A_2 \leftarrow X\,^2B_1$ transition of OClO and $A\,^2\Pi \leftarrow X\,^2\Pi$ transition in ClO allow removal of the spectral contributions of these species by scaling reference spectra and subtracting them from the mixed spectrum to reveal underlying broad band features.

The DAS used was a Jobin-Yvon CP200 instrument, operated by QUIK-VIEW software installed on a 486-SX PC. A 360 groove mm^{-1} holographically etched grating was employed in a dedicated spectrograph; the resolution was *ca.* 1.5 nm (FWHM) when coupled with an entrance slit width of 50 μm. The UV light source was a 50 W Hammamatsu deuterium lamp mounted in an Oriel lamphouse fitted with a rear reflector. The output from the lamphouse was partially collimated by passing it through two plano-convex quartz lenses. The light beam was passed through an iris diaphragm before entering the collimation system of the detector. The wavelengths quoted throughout this paper are those appropriate to air at 1 atm, although at the resolution here there is no significant difference from wavelengths in vacuum.

A schematic diagram of the experimental set up is shown in Fig. 1. A path length of 10.5 cm was obtained from a single pass through a quartz crosspiece (i.d. 30 mm) attached at right-angles to the direction of flow down a conventional quartz flow-tube (i.d. 38 mm) fitted with a sliding injector. Quartz discs (Suprasil-A; 3 mm thick, 35 mm diameter) were attached to the ends of the crosspiece as optical windows. A Leybold rotary vacuum pump, fitted with a Roots Blower, was used to maintain the flow down the flow-tube, which was attached to a conventional gas handling manifold to allow manipulation of gases.

The flow-tube used in this study could be operated over the temperature range 220–320 K. The temperature was controlled *via* two independent type-T thermocouples, each connected to a temperature controller (RS Cal 9900 PID). One thermocouple was attached to the crosspiece of the cell, and the other to the main body of the tube. Two thermofoil ribbon heaters were used to heat the crosspiece and main tube body to a temperature determined by the controller units. Copper foil wrapped around the crosspiece and flow-tube body was employed to smooth out the temperature profile along the tube; this profile was verified using a surrogate sliding injector fitted with a Type-T thermocouple. Seven additional thermocouples, six along the body of the tube, and one on the crosspiece, provided additional information on the temperature profile of the tube while experiments were in progress.

Reduced-temperature operation was achieved by surrounding the flow-tube and crosspiece with solid CO_2. The entire tube was enclosed in a plastic box, insulated with polystyrene foam. Since most of the experimental work was carried out at or below room temperature, the temperature profile of the flow-tube was optimised for work at low temperatures by moving coils of heating tape in response to hot and cold spots revealed by the sliding-injector thermocouple. At a set-point of 243 K, the temperature profile along the tube was constant to within ~1 K; the error in the temperature profile increased to around ~3 K for temperatures below, but approaching, room temperature. At 320 K, the excursions were of the order of ~10 K.

Condensation on the optical windows of the crosspiece was avoided by attaching secondary windows to the crosspiece with a silicone sealant. The secondary windows protruded beyond the plastic box, and the spaces between the crosspiece windows and the secondary windows were evacuated with a small rotary pump. This arrangement was successful in avoiding condensation, but increased the distance between the UV light source and the detector by an additional 25 cm.

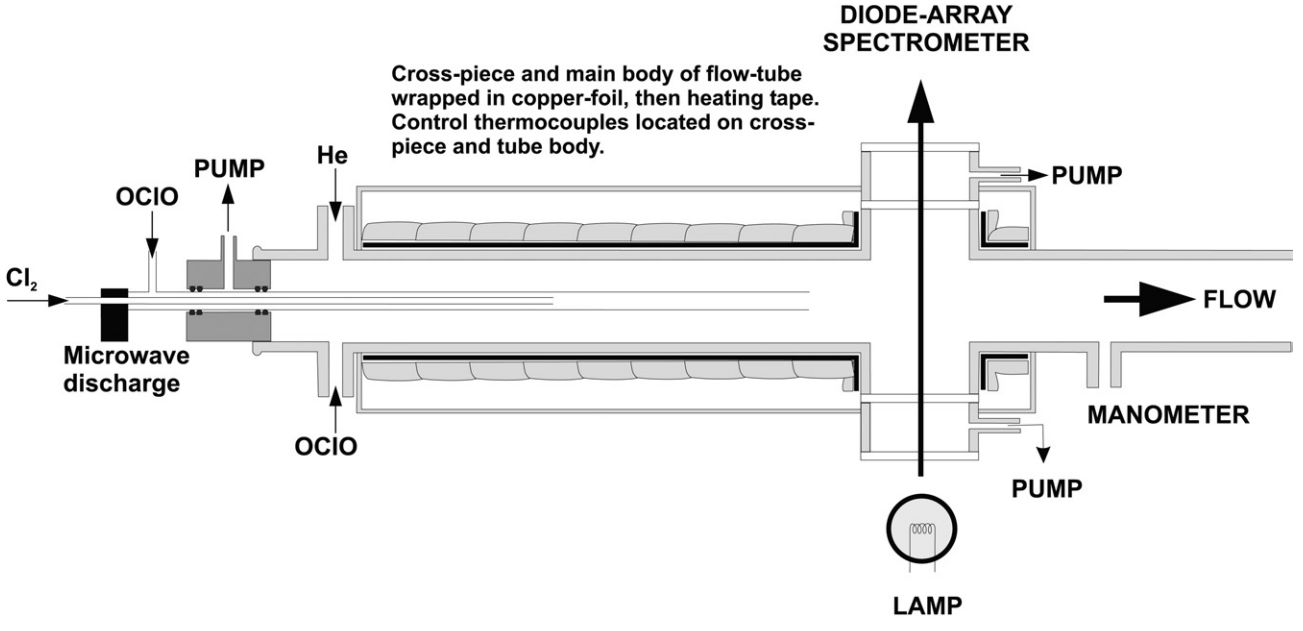

Fig. 1 Diagrammatic representation of the key parts of the flow-tube used in the determinations of cross sections. A path length of 10.5 cm was obtained from a single pass through a quartz crosspiece (i.d. 30 mm) attached at right-angles to the direction of flow down a conventional quartz flow-tube (i.d. 38 mm).

Reagents and syntheses

Precursor reagents were manipulated using the gas-handling manifold. Chlorine was used as supplied by BDH (99.99%), with freeze–pump–thaw cycles being used for purification. OClO was made as required using the method of Derby and Hutchison[14] in a purpose-built synthesis rig. The formalised reaction is

$$\tfrac{1}{2}Cl_2 + NaClO_2 \rightarrow OClO + NaCl \quad (1)$$

The effluent from the $NaClO_2$ (BDH, technical grade) was dried by passing the gas over a bed of P_2O_5. No evidence for contamination by CO_2 or H_2O was found on analysing a sample of OClO with FTIR spectroscopy. However, quantitative conversion of Cl_2 to OClO could not be achieved. We suspect that some Cl_2 is lost on the moist $NaClO_2$ beds. If the $NaClO_2$ was used dry from the container, OClO production ceased after a few minutes, but could be restarted by lightly moistening the $NaClO_2$ again. Moisture thus seems to be an essential component, implying that the reaction is considerably more complex than eqn. (1) would suggest. More detail is provided in a paper by us describing the oxides Cl_2O_4 and Cl_2O_6.[15]

ClO, when required for formation of Cl_2O_3 in reaction (2)

$$ClO + OClO + M \rightleftharpoons Cl_2O_3 + M \quad (2)$$

was produced by the reaction of Cl atoms with OClO. Reaction took place in the sliding injector of the flow-tube, Cl atoms being produced by the action of a microwave discharge through a mixture of Cl_2 and He. Cl_2O_3 formation is favoured by low temperatures, so that the synthesis usually took place with the flow-tube held at $T = 243$ K and at pressures of up to 10 Torr. Although we have isolated Cl_2O_3 in the low-temperature photolysis of OClO with a Xe-arc lamp, it is contaminated with other species, including chloryl chloride. Cl_2O_3 exhibits considerably greater thermal instability than Cl_2O_6 and Cl_2O_4; we were not able to synthesise large enough quantities to use the same approach with Cl_2O_3 as that taken for the other oxides.[15] Cl_2O_3 was therefore synthesised by allowing ClO to combine with OClO in the main body of the flow-tube. ClO dimer formation

$$ClO + ClO + M \rightleftharpoons Cl_2O_2 + M \quad (3)$$

is a process that competes for loss of ClO at the low temperatures used in the formation of Cl_2O_3. However, the rate coefficient for reaction (3) is about five times smaller under the conditions used than that for reaction (2), and the contribution of the dimer was further reduced by working with high concentrations of OClO.

While the flow-tube was being used to synthesise gas-phase Cl_2O_3, UV absorptions due to Cl_2, OClO, ClO and Cl_2O_3 could all be discerned. Some contribution due to Cl_2O_2 was almost certainly present, but, as discussed later, the absorption was insignificant compared to that of the Cl_2O_3. The Cl_2 absorption peaks at $\lambda_{max} = 333$ nm and underlies the structured absorption of OClO. The absorption of ClO overlies that of the absorption due to Cl_2O_3.

Methodology of spectral acquisition and manipulation

Alteration of contact time between the reactants by moving the sliding injector was the routine procedure in the kinetic experiments. It was also used to verify that the chemical system had reached equilibrium in the determinations of the equilibrium constant for reaction (2). In our system, particularly at the lower temperatures studied, the grease (Fomblin) used to lubricate the O-rings sealing the main sliding injector became very viscous. This viscosity in turn caused resistance to movement which resulted in sliding injector movement transferring to the optical windows. In an optical system such as ours, the spectral baseline is very sensitive to such movement and considerable variations in baseline were caused by movement of the sliding injector. At each injector position, therefore, spectra were obtained with the microwave discharge excited and extinguished (Fig. 3: panels (a) and (b) show these spectra for two injector positions). Subtraction of the second spectrum from the first resulted in a new composite spectrum with no baseline fluctuations, positive contributions from Cl_2O_3 and ClO and a negative contribution from ClO and OClO (spectra (c) and (d) of Fig. 3). The considerable amount of Cl_2 present in the two original spectra largely cancels out as only a small fraction of the Cl_2 initially added is converted to Cl atoms that are lost by reaction when the discharge is excited. Changes in concentration of OClO at a fixed contact time were also used to alter the equilibrium of the chemical system. This method was used in the determination of the Cl_2O_3 absorption cross sections, where an increase in the OClO concentration was matched to a loss of ClO and gain in Cl_2O_3 (the exact stoicheiometry is discussed later).

In the kinetic experiments, a minimum distance (d_0) between the tip of the sliding injector and the observation cell was used to establish satisfactory mixing of the injected reactant. An estimate of the minimum acceptable distance was obtained by adding a flow of OClO to the flow of carrier gas in the flow-tube operating in the normal pressure regime. As the injector was moved closer to the cell, the absorption due to OClO remained constant until a critical position was reached, and it was assumed that the tip distance then corresponded to d_0 (not less than 10 cm in our system). This distance thus defines 'zero time' (t_0) for the kinetic experiments. Unfortunately, significant amounts of ClO were lost to form Cl_2O_3 between the injector tip and the observation cell, thus adding some complication to the analysis of the data.

Spectral stripping of OClO presented us with some problems. Our diode-array was automatically cooled to $-20\,^{\circ}C$ to reduce the contribution of thermal noise from the diodes. Thermal instability in the system meant that some small shifts in the convoluted line shape of OClO were unavoidable. Thus, although we recorded OClO reference spectra frequently, some mismatching of reference and experimental spectra occurred at peak maxima and minima. This resulted in some 'ghosting' even in our best efforts to strip OClO, which can be seen, for example, on the noisier spectrum shown in Fig. 2. This inability to remove OClO completely from our composite spectra results in our conservative error estimates for measurements involving the spectral regions affected by the OClO structure, detailed later.

Measurement of the absorption cross section of Cl_2O_3

The general procedure for the measurement of the absorption cross section for Cl_2O_3 in the discharge-flow system has just

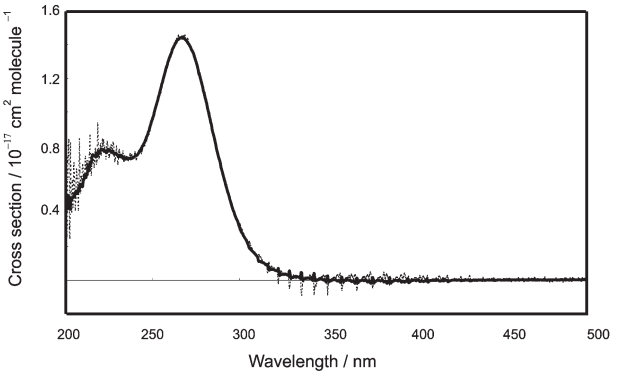

Fig. 2 Absorption spectra of Cl_2O_3: (—) high S/N ratio, (---) lower S/N ratio, high accuracy cross section (see text).

been outlined. The DAS technique permits scaling and subtraction of spectral components from a composite spectrum, so that if the contributions of Cl_2, OClO and ClO are quantified, the 'pure' spectrum of Cl_2O_3 can be extracted. Concentrations of OClO in the system were varied in order to force changes in the equilibrium concentrations of Cl_2O_3. The concentration of the Cl_2O_2 dimer is relatively unaffected by the addition of OClO, although a consequence of the loss of ClO to form Cl_2O_3 is a shift in the equilibrium of reaction (3) to release ClO. Thus some of the Cl_2O_2 will be lost and the ClO freed to be sequestered as Cl_2O_3. Kinetic modelling of the reactions shows that approximately 4% more Cl_2O_3 was formed than the difference in [ClO] and a 1:1 stoichiometry for reaction (2) would imply.

By recording consecutive experimental spectra with low and high concentrations of OClO and then subtracting the spectrum with high [OClO] from that with lower [OClO], a difference spectrum is obtained in which the contribution of Cl_2 cancels out, and that of the Cl_2O_2 essentially does also. This difference spectrum has negative contributions from OClO and ClO, and positive ones from Cl_2O_3. Since Cl_2O_3 is a broad-band absorber, the structure in this difference spectrum is due only to ClO and to OClO. The structure thus provides an easy method of quantifying the concentrations of ClO and OClO, using the Beer–Lambert law, and the (temperature-dependent) absorption cross sections measured using the same flow-tube and spectrometer. Reference spectra were scaled to the negative absorbances of ClO and OClO, and then added to the difference spectrum. The result was a spectrum containing an absorption due only to Cl_2O_3 (and a small negative contribution from loss of Cl_2O_2): see panels (e) and (f) of Fig. 3. In practice, the scaling and addition was achieved with an 'in-house' computer program.

Two sets of experiments were carried out. The first set was carried out at low ClO concentrations to minimise the amount of Cl_2O_2 formed (and then subsequently lost). From this set of experiments, we obtained the most reliable value for the absolute absorption cross section at $\lambda_{max} = 267$ nm of Cl_2O_3. Due allowance was made for the small contribution (*ca.* 4%) to [Cl_2O_3] beyond that implied by 1:1 stoicheiometry for reaction (2); the exact contribution was calculated from the kinetic model. This cross section was then used to scale a relative spectrum resulting from experiments conducted at higher ClO concentrations, which had a substantially improved signal-to-noise ratio. The second spectrum was a smooth fit through the noisier first spectrum (Fig. 2) since the absorption contribution due to Cl_2O_2 is small. The kinetic modelling of the system shows that the actual predicted contribution of the Cl_2O_2 to the difference spectrum in the first experiments is approximately 2×10^{-5} absorbance units whereas the noise on the spectrum at $\lambda = 267$ nm is about $\sim 5 \times 10^{-4}$ absorbance units.

Effective cross sections of OClO and ClO

The procedure just outlined evidently requires a quantitative knowledge of the absorption spectra of the species other than Cl_2O_3 present in the system. There are, however, potential problems, since the absorption cross sections of OClO and of ClO in the structured part of its spectrum are highly dependent on instrument resolution and temperature.[13,16] The paragraphs that follow explain how we obtained spectral data appropriate to the resolution and temperature of our experiments. In the case of OClO, we decided to measure the absorption cross section of OClO directly in our system. Small quantities of OClO were condensed in a cold finger at a temperature of 77 K; the trap was warmed to 196 K and Cl_2 pumped off. The OClO was then allowed to evaporate into the flow-tube and the absorption cross section was determined by making measurements

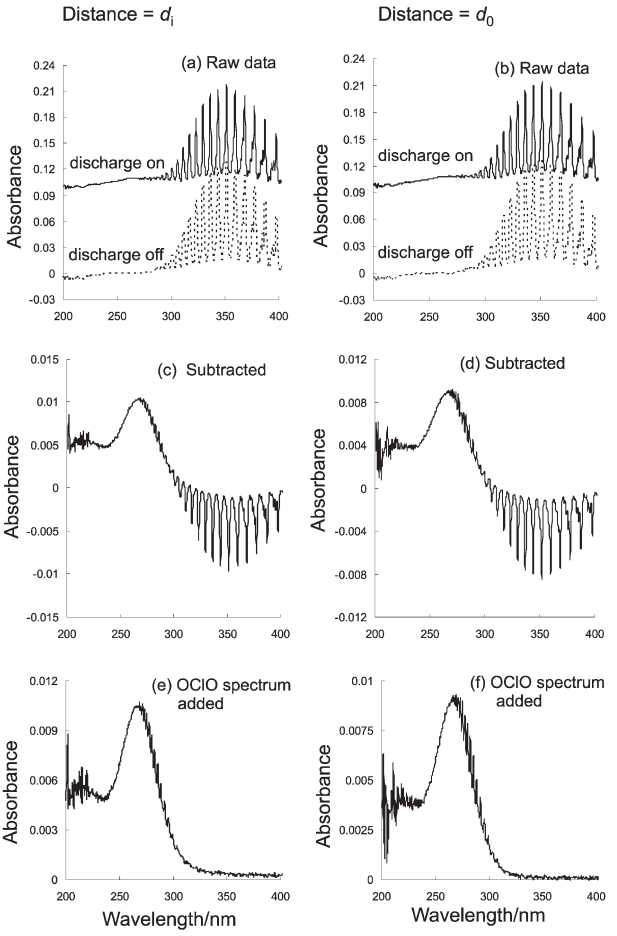

Fig. 3 Manipulation of spectra for kinetic study. Panels (a) and (b) show the raw spectra at a distance d_i and at 'zero' injector distance, d_0, with the microwave discharge on (—) and off (---). The 'discharge-on' spectra have been offset by 0.10 absorbance units for clarity of presentation. Panels (c) and (d) show the results of subtraction of the 'discharge-off' spectrum from the 'discharge-on' spectrum. Panels (e) and (f) show the effect of adding a scaled reference OClO spectrum to eliminate the negative OClO absorbance present in the middle two panels.

in pairs, one with a high concentration of OClO, the other with a low concentration. The two spectra were then subtracted from each other, as were the corresponding pressures. The pressure in the flow-tube never exceeded 3 Torr and the gases were assumed to be ideal, allowing a calculation of the number density in the sample from the difference in pressures. Absorbances were measured in this way for several concentrations of absorber, and the cross sections calculated using the known optical path. The experimental method was verified using a flow of Cl_2, regulated with a flowmeter and a needle-valve. The resulting cross section was in good agreement with the value currently recommended.[13]

Measurements were made with the flow-tube at a range of different temperatures and the results are shown in Fig. 4. The cross sections reported on this figure represent the *differences* between the peak absorption at $\lambda = 351.3$ nm and trough at $\lambda = 357.5$ nm. The equivalent differences derived from the measurements of Kromminga *et al.*[16] for a resolution of 20 cm^{-1} are shown for comparison; but it must be remembered that identical values are not anticipated because of the different instrumental behaviour. Our procedure for determining the effective cross sections for ClO was rather different, and depends on the spectrum possessing structure at wavelengths greater than *ca.* 270 nm, but displaying only a continuum at shorter ones. Fortunately, the absorption cross section in the continuum is independent of temperature.[13] Initially, we used

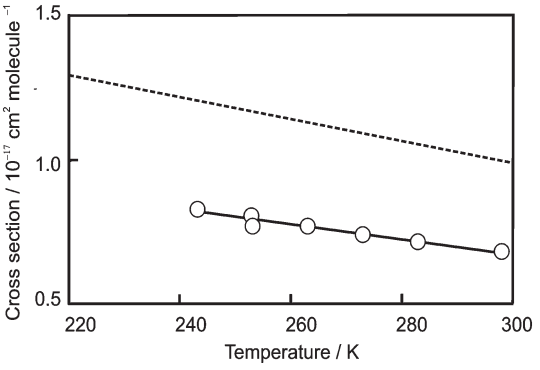

Fig. 4 Effective absorption cross section of OClO as a function of temperature: (○) this work, (---) current NASA/JPL recommendation (Sander *et al.*, 2003).[13] The cross sections reported on this figure represent the *differences* between the peak absorption at $\lambda = 351.3$ nm and trough at $\lambda = 357.5$ nm.

the reaction

$$Cl + O_3 \rightarrow ClO + O_2 \quad (4)$$

as a source of ClO in order to measure the absorption cross section at the peak of the continuum ($\lambda = 265$ nm). Atomic chlorine, generated by passing a microwave discharge through Cl_2 diluted in He, was added in the flow system to an excess (*ca.* 10 times) of O_3, and the consumption of O_3 determined from the changes in optical absorption at $\lambda = 254$ nm. On the assumption of 1:1 stoicheiometry for reaction (4), we obtained a first estimate of $\sigma = 5.2 \times 10^{-18}$ cm^2 molecule^{-1}. Since this value is the same as that recommended[13] on the basis of much more extensive measurements, we took it merely as a confirmation that the recommendation was appropriate for use in our system. When other absorbers are present, as in the experiments on Cl_2O_3, it is, of course, the *structured* region of the ClO absorption that provides the best indication of concentration. For our purposes, the difference between the peak absorbance and the trough absorbance was summed for the eight principal peaks of the ClO spectrum. It must be noted that the structured spectrum of ClO is not symmetric about the wavelength of maximum absorption (*ca.* 275 nm). Thus, if there is an absorption underlying a ClO spectrum, the magnitude of the difference between the peaks and troughs is dependent to some extent on the amount of distortion introduced by that absorber (and therefore on its concentration). To ensure that measurements of the structure of the ClO spectrum depended only on the concentration of the ClO, a computer routine was written that would fit a fourth-order polynomial to the spectrum. Such a low-order polynomial applied to the spectrum for $\lambda = 255$–290 nm cannot follow the structure (at our instrumental resolution), and thus produces a smooth average through it. By subtracting the polynomial function from the structured spectrum, a difference spectrum is obtained that contains only the structure of the ClO and is independent of any amount of distortion by underlying broad-band absorbers. To get a true concentration of ClO, the amount of structure determined in this manner then had to be related to the amount of broad-band absorbance at $\lambda = 265$ nm. For a given temperature and instrument resolution, the ratio of the absorbance at $\lambda = 265$ nm to that of the summed difference peak–trough absorbance, δ, should be a constant. Examination (by means of a computer program) of the pure reference spectrum of ClO allowed a structure-to-broad-band absorbance ratio to be obtained for each temperature. Application of this ratio to the value of δ determined in a spectrum of ClO with another broad-band absorber present allowed the magnitude of the ClO absorbance at $\lambda = 265$ nm to be found, thus yielding the concentration of ClO to be found in the mixture spectrum. The reference spectrum can then be scaled to remove the ClO contribution from the experimental spectrum.

Equilibrium constant for reaction (2)

In the temperature range of the experiments (243–298 K), the concentration of the three species in reaction (2) could be determined by the methods outlined earlier. To ensure that the system was at equilibrium, the contact time of the reactants in the flow-tube was increased by withdrawing the sliding injector until the concentration of the three species remained constant. As in the other experiments described in this paper, reference measurements were made in each run with the microwave discharge extinguished. At each temperature, the equilibrium constant was calculated from the concentrations of ClO, OClO and Cl_2O_3 present in the flow for six different initial concentrations of added OClO.

Rate coefficient for the formation of Cl_2O_3

OClO was produced through the reaction of Cl_2 with $NaClO_2$ (reaction (1)), and introduced into the flow-tube through a side arm. ClO was produced in the sliding injector through the reaction of Cl atoms from a microwave discharge through Cl_2 with a separate supply of OClO in the process

$$Cl + OClO \rightarrow ClO + ClO \quad (5)$$

Titration of the Cl atoms with OClO ensured that the reactive species leaving the tip of the sliding injector were mainly ClO and Cl_2. The carrier gas was He, which constituted the bulk of the flow.

At temperatures below 243 K and at a total pressure of approximately 2 Torr, a colourless condensate formed in the flow-tube. It was not possible to ascertain the identity of the condensate because it also condensed on the windows of the absorption cell, reducing the transmission of the light through scattering. We believe that the condensate was probably Cl_2O_3 in the light of experiments conducted separately.[15] Scattering of the probe beam by the condensate prevented us from conducting experiments below $T = 243$ K. Above $T = 283$ K, the concentration of Cl_2O_3 formed was so small that our signal-to-noise ratio was insufficient to perform kinetic measurements.

Kinetic measurements were carried out by recording UV absorption spectra for a series of six injector distances, which corresponded to six contact times. An 'in-house' computer program generated the difference of the spectra obtained with and without the microwave discharge excited, and then added a scaled reference OClO spectrum, to produce a spectrum that contained only absorptions due to ClO and Cl_2O_3 (see Fig. 3, panels (e) and (f)). The concentrations of ClO and Cl_2O_3 were obtained from this spectrum using the methods described previously. The concentration of OClO could be obtained in a similar manner from the spectrum obtained when the microwave discharge was excited. 'Zero' injector distance spectra with the microwave on and off were recorded before each new injector distance was set and were used to calculate the initial concentrations of ClO, OClO and Cl_2O_3 for each contact time.

Results and discussion

The absorption cross section of Cl_2O_3

The absorption cross section of Cl_2O_3 at $\lambda = 267$ nm was determined by the method described in the experimental section to be $(1.44 \pm 0.10) \times 10^{-17}$ cm^2 molecule^{-1}, a value that may be compared to the recommended value of 1.68×10^{-17} cm^2 molecule^{-1} adopted in recent data compilations.[13] The errors quoted are twice the standard deviations of the

absorbance-concentration plots used to derive the cross section at $\lambda_{max} = 267$ nm, taken together with estimates of systematic errors. Table 1 lists the absorption cross section as a function of wavelength at one nm intervals between $\lambda = 201$ nm and $\lambda = 320$ nm, interpolated from the raw data using a cubic spline fit. Although systematic errors may be associated with the calculation of the amount of ClO lost, as quantified numerically, the kinetic studies suggest that there is not any hitherto unsuspected chemistry occurring. At wavelengths greater than λ_{max}, the spectral-stripping procedure leaves small 'spikes' due to OClO, as explained in our Experimental section. As a result, errors at the longer wavelengths will be substantially greater than at λ_{max}: we estimate the error limits to be ~35% at 320 nm.

Table 1 Absorption cross section of Cl_2O_3 as a function of wavelength

Wavelength/ nm	$\sigma/10^{-17}$ cm^2 molecule^{-1}	Wavelength/ nm	$\sigma/10^{-17}$ cm^2 molecule^{-1}
201	0.44	261	1.36
202	0.45	262	1.39
203	0.49	263	1.41
204	0.49	264	1.43
205	0.49	265	1.43
206	0.53	266	1.44
207	0.54	267	1.44
208	0.57	268	1.44
209	0.57	269	1.43
210	0.59	270	1.41
211	0.63	271	1.40
212	0.63	272	1.38
213	0.67	273	1.36
214	0.70	274	1.33
215	0.72	275	1.30
216	0.74	276	1.25
217	0.74	277	1.21
218	0.75	278	1.18
219	0.75	279	1.14
220	0.77	280	1.10
221	0.77	281	1.05
222	0.77	282	1.00
223	0.76	283	0.96
224	0.78	284	0.91
225	0.77	285	0.87
226	0.76	286	0.82
227	0.76	287	0.77
228	0.75	288	0.73
229	0.75	289	0.69
230	0.74	290	0.65
231	0.74	291	0.61
232	0.74	292	0.57
233	0.72	293	0.53
234	0.72	294	0.50
235	0.72	295	0.46
236	0.72	296	0.43
237	0.72	297	0.40
238	0.72	298	0.37
239	0.73	299	0.35
240	0.74	300	0.32
241	0.74	301	0.29
242	0.76	302	0.27
243	0.77	303	0.25
244	0.80	304	0.24
245	0.81	305	0.21
246	0.84	306	0.19
247	0.86	307	0.18
248	0.89	308	0.17
249	0.93	309	0.16
250	0.96	310	0.14
251	1.00	311	0.11
252	1.04	312	0.11
253	1.07	313	0.11
254	1.11	314	0.10
255	1.15	315	0.09
256	1.19	316	0.10
257	1.23	317	0.06
258	1.27	318	0.06
259	1.3	319	0.06
260	1.33	320	0.06

Quite a wide range of spectral shapes and values of the absorption cross section for Cl_2O_3 at λ_{max} have been reported. Some representative measurements are compared with ours in Fig. 5. There is reasonably good agreement within the limits of errors that we have quoted. However, we would humbly suggest that our central value from the new determination could more closely approach the true one because the methodology that we have adopted has been designed to reduce contributions from species adventitiously present and to minimize spectral contamination by use of the possibilities for stripping and manipulation afforded by the use of the DAS.

We regard it as an important point of our experiments that the use of the multiplex DAS means that the *relative* spectrum obtained is likely to be of high precision, regardless of the assumptions made about absolute concentrations, and the only likely cause of errors in the shape of the spectrum would be the presence of unknown absorbers for which allowance had not been made.

One striking feature of the comparison presented in Fig. 5 is that the early quantitative flash-photolysis experiments of Lipscomb *et al.*[8] not only suggested the existence of Cl_2O_3, but also provided an absorption cross section not far removed from the values now under consideration. Examination of the figure will show that the shape of our spectrum matches the spectrum measured by Burkholder *et al.*[11] more closely than it does those of Harwood *et al.*[12] or Hayman and Cox,[9] and the agreement of the cross section at λ_{max} is good as well. The absence of long- or short-wavelength 'tails' in our spectrum is possibly of significance, because it is the absence of these features that differentiates the spectrum of Burkholder *et al.*[11] from the others, and that stimulates Sander *et al.*[13] to remark that "additional work is needed". From the point of view of potential atmospheric importance, it may be the differences in the region beyond $\lambda = 300$ nm that have the largest impact, although Fig. 5 shows that the disagreements between the different authors are most pronounced at wavelengths shorter than λ_{max} (where other chlorine oxides would be likely to make the most significant relative contribution).

Our experiments reported here differ from all others published in that we did not employ a photochemical source of

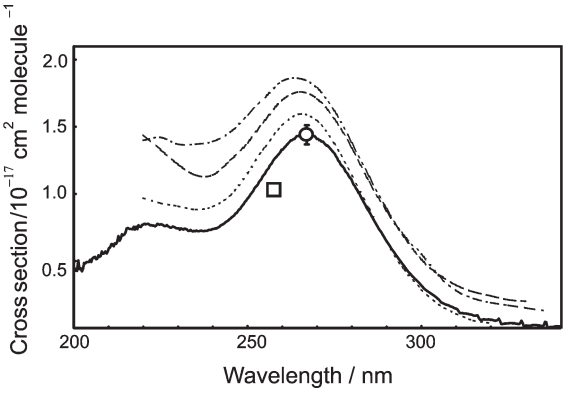

Fig. 5 Comparison of selected measurements of the absorption cross section of Cl_2O_3: (—) this work, (○) this work, absolute value and associated errors used at $\lambda = 257$ nm to scale spectrum; (···) Burkholder *et al.* (1993),[11] (---) Harwood *et al.* (1995),[12] (–·–) Hayman and Cox (1989),[9] (□) Lipscomb *et al.* (1955).[8]

Cl_2O_3. We draw attention to this distinction, because there exists at least the possibility that other absorbers might be formed in a way not anticipated in some of the photochemical systems that have been used. Systems in which both O and OClO are present simultaneously seem particularly prone to this problem. Some absorber is undoubtedly formed, as observed both by ourselves[15] and others.[6,12] Recognition of the possibility of some interference led Hayman and Cox[9] to attempt to scavenge the O atoms by arranging for the presence of an excess of O_2, but they may have been only partially successful in removing the atoms.[6] Burkholder *et al.*[11] used an elaborate alternative photochemical procedure to obviate the need for photolysis of OClO in generating ClO, and it is therefore instructive that the spectrum of these workers corresponds most closely with ours. Parr *et al.*[10] suggested that the differences between their spectrum and that of Hayman and Cox[9] could be explained by the formation of Cl_2O_4 in the earlier experiments, although the improved spectrum[15] of Cl_2O_4 suggests that the presence of this oxide cannot be the sole cause of the differences. Several other molecules are potential absorbers, including ClO_3, which might be formed in the reaction of O with OClO, and chloryl chloride, $ClClO_2$, which may be generated in the photolysis of mixtures of OClO with Cl_2.[15] In view of the suspicion that thus attends some of the photochemical methods that have hitherto been used for production of Cl_2O_3, the thermal technique adopted in the present experiments commends itself as a useful alternative.

The equilibrium constant as a function of temperature

The equilibrium constants K_c for reaction (2) were calculated from the concentrations and converted to values of K_p for each temperature. Values of K_c and K_p are listed in Table 2: each is the average of six separate determinations. Fig. 6 displays K_p as a function of temperature in the form of a van't Hoff plot. A linear regression through the data allowed the thermodynamic parameters $\Delta_rH^{\ominus}$ and $\Delta_rS^{\ominus}$ for reaction (2) to be determined from the gradient and intercept. Values of $\Delta_rH^{\ominus} = -57.9 \pm 2.1$ kJ mol^{-1} and $\Delta_rS^{\ominus} = -132.6 \pm 7.9$ J K^{-1} mol^{-1} were obtained. The error limits given here and throughout the thermochemical discussion that follows refer to two standard deviations of the statistical contribution.

Also shown in Fig. 6 for comparison are the equilibrium data of Hayman and Cox[9] from which a value of $\Delta_rH^{\ominus} = -62 \pm 12$ kJ mol^{-1} and $\Delta_rS^{\ominus} = -151 \pm 50$ J K^{-1} mol^{-1} was obtained, and of Burkholder *et al.*[11] from which a value of $\Delta_rH^{\ominus} = -46.4 \pm 5.0$ kJ mol^{-1} and $\Delta_rS^{\ominus} = -88.6 \pm 18.8$ J K^{-1} mol^{-1} was obtained. Burkholder *et al.*[11] obtained their values by combining their data with the data of Hayman and Cox,[9] but excluding their measurement at $T = 233$ K. Examination of Fig. 6 shows that our data provide a good fit to a straight line, and include points at two higher temperatures than do the other two sets. Although a van't Hoff plot does not necessarily have to be perfectly linear, the smaller scatter on our data compared with those of other workers, and the extension to higher temperatures, suggests that reliance may be placed on our central values of $\Delta_rH^{\ominus}$ and $\Delta_rS^{\ominus}$.

Table 2 The equibrium constant K_p and K_c for reaction (2) as a function of temperature

Temperature/K	K_p/atm^{-1}	K_c/cm^3 molecule^{-1}
243	3.14×10^5	1.04×10^{-14}
253	1.03×10^5	3.54×10^{-15}
263	3.93×10^4	1.41×10^{-15}
273	1.37×10^4	5.11×10^{-16}
283	5.99×10^3	2.31×10^{-16}
298	1.55×10^3	6.29×10^{-17}

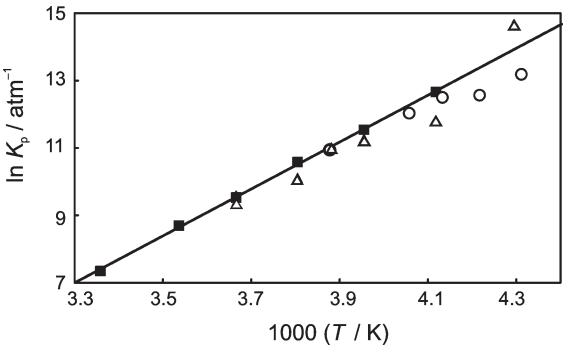

Fig. 6 A van't Hoff plot of equilibrium constant data. The closed squares (■) represent our data. The open circles (○) represent the data of Burkholder *et al.* (1993),[11] whilst the open triangles (△) represent the data of Hayman and Cox (1989).[9] The solid line is a least squares fit through our data.

Evidence for this assertion is provided by the Third-Law analysis carried out by Burkholder *et al.*[11] $\Delta_rS^{\ominus}$ was calculated by statistical mechanics at each temperature for which K_{eq} was determined experimentally. $\Delta_rH^{\ominus}$ was then obtained from the resulting values of $\Delta_rG^{\ominus}$ together with $\Delta_rS^{\ominus}$. The Third-Law method is generally preferred over the van't Hoff (Second-Law method) in analysing equilibrium constant data if molecular constants for the equilibrium species are accurately known. Burkholder *et al.*[11] used molecular constants from Herzberg and Huber[17] and Pillai and Curl[18] for ClO and OClO respectively. Rotational constants and ground electronic state degeneracy of Cl_2O_3 were obtained from the data of Friedl *et al.*[19] Experimental determinations of the vibrational frequencies of Cl_2O_3 have yet to be made. Consequently, vibrational frequencies for Cl_2O_3 were obtained from the *ab initio* calculation of Hehre,[20] communicated privately. By assuming that the lowest vibration of Cl_2O_3 was a free rotation, Burkholder *et al.*[11] calculated a value of $\Delta_rS^{\ominus} = -120.8$ J K^{-1} mol^{-1} between 232 and 258 K, which was some 26% higher than the value they determined through the Second-Law analysis, and significantly outside the error limits. They attributed the difference to uncertainties in the understanding of the spectroscopy of Cl_2O_3. However, the value of $\Delta_rS^{\ominus}$ obtained from the Third-Law analysis is within 10% of the value obtained from our Second-Law analysis. This value of $\Delta_rS^{\ominus}$ can be used to calculate values of $\Delta_rH^{\ominus}$ at temperatures for which the equilibrium constant has been determined. The Third-Law values of $\Delta_rH^{\ominus}$ calculated by Burkholder *et al.*[11] were again significantly higher than those given by their Second-Law determinations. Assuming that $\Delta_rS^{\ominus}$ remains independent of temperature up to $T = 298$ K, the Third-Law value from Burkholder *et al.* can be applied to our equilibrium constants (and corresponding values of $\Delta_rG^{\ominus}$) to obtain $\Delta_rH^{\ominus}$ for each temperature. These results are shown in Table 3. Examination of the calculated values of $\Delta_rH^{\ominus}$ shows that they are within about 6% of the value obtained (-57.9 ± 2.1 kJ mol^{-1}) from the Second-Law analysis of our data. The self-consistent results thus give us further confidence in our experimentally determined values of $\Delta_rH^{\ominus}$ and $\Delta_rS^{\ominus}$.

Table 3 Third-law analysis of equilibrium-constant data

Temperature/K	$\Delta_rG^{\ominus}$/kJ mol^{-1} Experimental	$\Delta_rS^{\ominus}$/J K^{-1} mol^{-1} Calculated	$\Delta_rH^{\ominus}$/kJ mol^{-1} Derived
243	−25.6	−120.8	−54.9
253	−24.3	−120.8	−54.8
263	−23.1	−120.8	−54.9
273	−22.6	−120.8	−54.6
283	−20.5	−120.8	−54.7
298	−18.2	−120.8	−54.2

We can also attempt to combine our equilibrium data with that of Burkholder *et al.*[11] and Hayman and Cox,[9] and perform a global linear fit on the data, assuming equal weighting for each data point. This analysis yields values of $\Delta_rH^\ominus = -54.3 \pm 6.1$ kJ mol^{-1} and $\Delta_rS^\ominus = -120.1 \pm 24.0$ J K^{-1} mol^{-1}. The central values are extremely close to the values obtained from the Third-Law analysis of our data. It might be argued that these values probably represent the most reliable experimental determination of the central values of $\Delta_rH^\ominus$ and $\Delta_rS^\ominus$ for reaction (2). However, because the error limits are significantly poorer than those for our data set alone, we are inclined to regard the values derived from this set ($\Delta_rH^\ominus = -57.9 \pm 2.1$ kJ mol^{-1} and $\Delta_rS^\ominus = -132.6 \pm 7.9$ J K^{-1} mol^{-1}) as the better approximation.

Using the values of $\Delta_rH^\ominus$ and $\Delta_rS^\ominus$ obtained from our Second-Law analysis, we can further calculate $\Delta_fH^\ominus$ and $S^\ominus$ for Cl_2O_3, using the values of $\Delta_fH^\ominus$ and $S^\ominus$ for ClO and OClO given in the latest thermochemistry evaluation by Sander *et al.*[13] The results are $\Delta_fH^\ominus = 138.3 \pm 2.4$ kJ mol^{-1} and $S^\ominus = 349.3 \pm 8.0$ J K^{-1} mol^{-1}, which differ substantially from the recommended values for Cl_2O_3 given by Sander *et al.*[13] of $\Delta_fH^\ominus = 150 \pm 6$ kJ mol^{-1} and $S^\ominus = 390 \pm 20$ J K^{-1} mol^{-1}. The recommended values given by Sander *et al.*[13] appear to be based solely on the thermodynamic data of Burkholder *et al.*,[11] which as just shown differ markedly from the results of the present determination. However, it should be noted that this recommendation is slightly different from the values given by Burkholder *et al.*[11] themselves. Furthermore, the reference for the recommendation points to a paper of Burkholder *et al.*[21] on nitric acid and not Cl_2O_3. Our thermodynamic data are more in line with the values of Hayman and Cox[9] and with those of previous evaluations. For example, Abramowitz and Chase[22] recommended values of $\Delta_fH^\ominus = 137.0 \pm 13$ kJ mol^{-1} and $S^\ominus = 325.62 \pm 5.0$ J K^{-1} mol^{-1}. We would also point to the recent theoretical work of Sicre and Cobos[23] who performed G3//B3LYP and G3//B3LYP/6-311+G(3d2f) level *ab initio* calculations on a range of chlorine oxides to determine $\Delta_fH^\ominus$. For Cl_2O_3, they obtained a value of $\Delta_fH^\ominus = 132.5 \pm 12$ kJ mol^{-1}, well within its own error limits of our experimental value.

Kinetics of formation of Cl_2O_3

The objective of this part of our study was to examine the kinetics of formation of Cl_2O_3 in the forward branch of the reaction

$$ClO + OClO + M \rightleftharpoons Cl_2O_3 + M \qquad (2, -2)$$

in the temperature range 243–283 K. At the pressures accessible in our experiments, the reaction is certainly in the low-pressure, third-order regime with M = He.[13] Our method depends on the simultaneous measurement using the DAS of [ClO], [OClO] and [Cl_2O_3]. Adequate signal/noise performance could be obtained for all three species only with a limited range of experimental conditions. In particular, it became evident that at higher pressures than about 2 Torr, ClO decayed too rapidly for accurate concentration measurements to be extracted from the UV absorption spectra. A determination of the dependence of reaction rate on [M] was thus precluded. Instead, rate coefficients were obtained at a fixed pressure of 2 Torr, corresponding to [M] = (6.8–7.9) × 10^{16} molecule cm^{-3} over the temperature range of the experiments. In this respect, our investigation is evidently more limited than that of, for example, Burkholder *et al.*,[11] but a comparison now becomes possible of the efficiencies of He and N_2 as third bodies in reaction (2).

$$\frac{d[Cl_2O_3]}{dt} = k_2[ClO][OClO][M] - k_{-2}[Cl_2O_3][M] \qquad (I)$$

The analysis of the experimental data in these experiments is made more complicated than usual in several ways. Although the concentration of OClO can be made to exceed that of ClO, a simple pseudo-first-order treatment is not valid if the decomposition process, reaction (−2), becomes significant, which it certainly will at the higher temperatures of our study. Some Cl_2O_3 has already been generated in our flow-tube by the shortest contact times at which we can make the spectroscopic observations, so that the full rate equation must be employed. Integration of this equation, with $k_{-2} = k_2/K_{eq}$, leads to a solution of the form

$$F(x) = k_2[M](t_1 - t_2) \qquad (II)$$

where

$$x = -([Cl_2O_3]_{t_1} - [Cl_2O_3]_{t_2}) \qquad (III)$$

$$F(x) = \frac{1}{\sqrt{B^2 - 4AC}} \ln\left\{\frac{2C + (\sqrt{B^2 - 4AC} - B)x}{2C - (\sqrt{B^2 - 4AC} + B)x}\right\} \qquad (IV)$$

and with

$$A = 1;\ B = [ClO]_{t_1} + [OClO]_{t_1} + 1/K_{eq};$$
$$C = [ClO]_{t_1}[OClO]_{t_1} - [Cl_2O_3]_{t_1}/K_{eq} \qquad (V)$$

A plot of $F(x)$ as a function of differential contact time, $(t_1 - t_2)$, should be linear, with a slope of k_2[M], and with zero intercept. Fig. 7 shows an example of such a plot for experimental data obtained at the lowest of the temperatures studied. The lower limit of temperature is set by condensation on the windows, and the higher limit by the sensitivity limit for measurement of [Cl_2O_3].

We thought it appropriate to test the competence of our method of analysis by subjecting to it 'synthetic' data generated by the FACSIMILE program using a selected input rate coefficient for k_2, and using reactant and product concentrations similar to those found experimentally. The trial yielded a derived rate coefficient within two per cent of the input value. Measured values of loss of ClO were sometimes different from those of x (gain in [Cl_2O_3]). This apparent lack of stoicheiometric behaviour was ascribed to losses of ClO in termolecular formation of the ClO dimer (favoured at low temperatures) or bimolecular reaction of ClO to form non-reactive products (favoured at high temperatures). The FACSIMILE models reproduced this behaviour. So long as OClO was in considerable excess over ClO, a condition imposed for the kinetic experiments, the predicted reaction stoicheiometry did not deviate by more than 10% from unity. Nevertheless, a small modification to the parameters A and B in eqn. (V) permitted a small empirical correction to be applied.

Table 4 presents the mean values of k_2 obtained for each temperature, the errors being the 95% confidence limits of the mean. As stated earlier, these values represent the

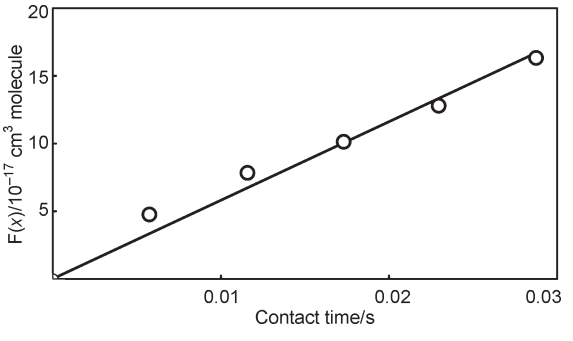

Fig. 7 $F(x)$ from eqn. (IV) plotted as a function of time for experimental data at $T = 243$ K. The solid line (—) represents a linear regression through the points with the intercept fixed at zero. The gradient of the linear regression yields the bimolecular rate coefficient.

Table 4 Rate coefficients for the formation and decomposition of Cl_2O_3 as a function of temperature

T/K	k_2/cm^6 molecule^{-2} s^{-1}	k_{-2}/cm^3 molecule^{-1} s^{-1}
243	$(7.1 \pm 0.4) \times 10^{-32}$	$(6.8 \pm 0.3) \times 10^{-18}$
253	$(5.9 \pm 0.3) \times 10^{-32}$	$(1.7 \pm 0.1) \times 10^{-17}$
263	$(5.0 \pm 0.3) \times 10^{-32}$	$(3.6 \pm 0.2) \times 10^{-17}$
273	$(4.2 \pm 0.3) \times 10^{-32}$	$(8.2 \pm 0.5) \times 10^{-17}$
283	$(3.7 \pm 0.6) \times 10^{-32}$	$(1.6 \pm 0.1) \times 10^{-16}$

low-pressure limiting rate coefficients, k_2^0, for the termolecular process. This being the case, the results may be fitted to the conventional inverse-exponential dependence on temperature

$$k_2^0(T) = k_2^0(300) \cdot (T/300)^{-n} \quad \text{(VI)}$$

Fig. 8 illustrates how our results follow this law closely by plotting ln $k_2^0(T)$ as a function of $(T/300)$. A non-linear least-squares fit to our data yields $k_2^0(300) = (2.8 \pm 0.1) \times 10^{-32}$ cm^6 molecule^{-2} s^{-1} and $n = -4.3 \pm 0.2$ (95% confidence limits) for He as the third body. These values can be compared with those of Burkholder *et al.*[11] of $k_2^0(300) = (6.2 \pm 1.0) \times 10^{-32}$ cm^6 molecule^{-2} s^{-1} and $n = -4.7 \pm 0.6$ (2σ error limits) for N_2 as the third body. The value of n is the same within error limits, showing that the temperature dependence of k_2^0 is the same with either third body. On the other hand, $k_2^0(300)$ is a factor of 2.2 larger for M = N_2 than for M = He, as might be expected on the basis of the relative efficiency of a diatomic and monatomic third body. Eqn. (VI), together with the factor of 2.2, predicts that $k_2^0(226) = 2.1 \times 10^{-31}$ cm^6 molecule^{-2} s^{-1} for M = N_2 at $T = 226$ K, a value that may be compared with the experimental determination of Parr *et al.*[10] of 2.8×10^{-31} cm^6 molecule^{-2} s^{-1} at the same temperature.

Kinetics of dissociation of Cl_2O_3

The rate coefficients obtained for the forward reaction (2) can be combined with the equilibrium constants K_{eq} determined in this work to calculate rate coefficients for the dissociation of Cl_2O_3 in reaction (−2). The values obtained are given in Table 4. Fig. 9 displays these results in Arrhenius form, and the rate equation derived from a non-linear least-squares fit is

$$k_{-2}^0 = (2.8 \pm 0.5) \times 10^{-8} \exp\{(-5370 \pm 50)/T\} \text{ cm}^3 \text{ molecule}^{-1} \text{ s}^{-1} \quad \text{(VII)}$$

for M = He, the errors being 95% per cent confidence limits. On the assumption that the nature of M influences the temperature-independent terms in eqns. (VI) and (VII) by equal factors, we can suggest an approximate form of eqn. (VII) for M = N_2 of

$$k_{-2}^0 = 6.2 \times 10^{-8} \exp(-5370/T) \text{ cm}^3 \text{ molecule}^{-1} \text{ s}^{-1} \quad \text{(VIII)}$$

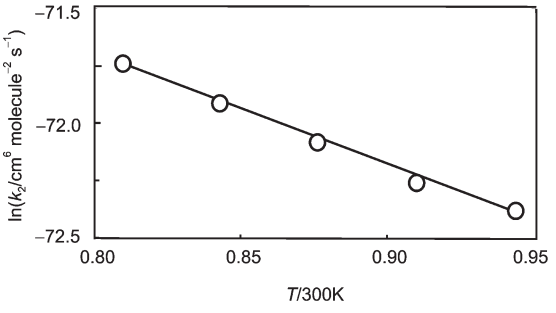

Fig. 8 Plot of ln k_2 as a function of $(T/300)$ for the association of ClO with OClO in reaction (2), with M = He for $T = 243$–283 K. The pressure was 2 Torr, and the reaction is in its low-pressure, third-order, regime at all temperatures.

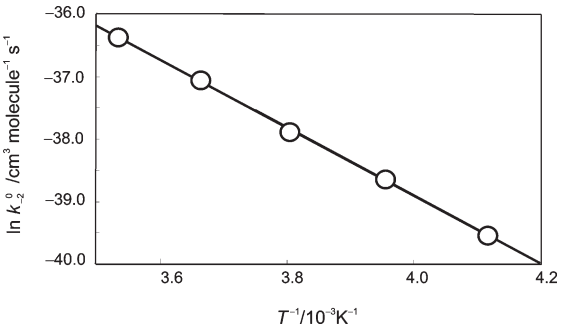

Fig. 9 Arrhenius plot for the dissociation of Cl_2O_3 in reaction (−2) with M = He for $T = 243$–283 K. The pressure was 2 Torr, and the reaction is in its low pressure, second-order, regime at all temperatures.

The most recent IUPAC data compilation[24] suggests a value for k_{-2}^0 of 2.8×10^{-18} cm^3 molecule^{-1} s^{-1} for M = N_2 at $T = 226$ K. Eqn. (VIII) yields a value of 3.0×10^{-18} cm^3 molecule^{-1} s^{-1}, although no particular significance should be attributed to the closeness of the match. More important, the IUPAC recommendation is for a single temperature, and has remained unchanged for more than a decade. It was based on the rate constant for the forward reaction (2) from Parr *et al.*[10] and the equilibrium constant of Hayman and Cox.[9] We suggest that the rate expression (VIII) could now reasonably replace the single-temperature recommendation, especially since the agreement at the common temperature is so good. It remains to point out that the only other previously published value of the rate coefficient and its temperature dependence, from Wongdontri-Stuper *et al.*,[3] is at variance with expression (VIII). Although the activation energy is similar, the pre-exponential factor appears to be too small by a factor of two orders of magnitude. It seems, then, that the indirect method of these workers was unable to provide a good approximation to the rate coefficient.

Eqn. (VIII) now makes possible a realistic extrapolation of the rate coefficient to conditions representative of the polar stratosphere, where the species Cl_2O_3 has been proposed on occasion as a reservoir of chlorine species. Previous attempts[10–12] to estimate the stratospheric lifetime were hindered by the lack of data suitable for extrapolation to temperatures below 200 K. For the conditions given by Burkholder *et al.*[11] as those most favourable for the formation of Cl_2O_3 ($P = 52$ mBar; $T = 187.5$ K), eqn. (VIII) predicts an effective pseudo-first-order rate constant of 0.04 s^{-1}, or a lifetime of around 25 s, half the earlier estimate of Parr *et al.*[10] for $P = 50$ mBar and $T = 190$ K (for which our calculated lifetime is *ca.* 16 s). According to the estimates of Parr *et al.*,[10] Burkholder *et al.*,[11] and Harwood *et al.*,[12] the lifetime of Cl_2O_3 against photolysis in the sunlit stratosphere would be more than 100 s. Thus, thermal decomposition of Cl_2O_3 always dominates over photolysis even under the conditions most favourable for photolysis, and the species will decompose rapidly even at night. As Burkholder *et al.* have pointed out, the build-up of significant concentrations of Cl_2O_3 in the stratosphere is unlikely, since OClO is a night-time species and ClO a daytime one. Only at dusk could elevated levels of Cl_2O_3 be formed, but they would decay within minutes, and essentially follow the time profile for disappearance of ClO, itself controlled largely by the rate of dimer formation.

Conclusions

The absorption cross section of Cl_2O_3 has been measured, and the present determinations are the first that have not used photochemical methods for the production of the molecule. Known impurities have been carefully quantified and the

appropriate corrections made. The shape of the spectrum is in better agreement with the data of Burkholder *et al.*[11] than with those of Harwood *et al.*[12] In particular, we concur with Burkholder *et al.*[11] in finding no long-wavelength tail such as that reported by Harwood *et al.*[12] in the region $\lambda = 300$–450 nm. It is possible that secondary O-atom chemistry interfered with the experiments of Harwood *et al.*[12] Our value of the absorption cross section at λ_{max} is in reasonable agreement with all previous determinations, although we report the lowest value of the cross section to date.

The equilibrium constant for the formation of Cl_2O_3 has been determined for a range of temperatures from 243 K to 298 K. A Second-Law analysis of the data allowed values of $\Delta_r H^{\ominus}$ and $\Delta_r S^{\ominus}$ to be determined. A composite van't Hoff plot can accommodate the previous measurements of both Hayman and Cox[9] and Burkholder *et al.*,[11] as well as those reported here, but our new data taken alone are less scattered (and more linear) than the combined data set. Thermodynamic values from both data sets are presented. A Third-Law analysis using the value of $\Delta_r S^{\ominus}$ of Burkholder *et al.*[11] also provides further support for the accuracy of our own measurement. Our thermodynamic data were also used to calculate values of $\Delta_f H^{\ominus}$ and $S^{\ominus}$ for Cl_2O_3, which are significantly different from the recommended values of Sander *et al.*[13]

The kinetics of the formation of Cl_2O_3 have been studied as a function of temperature between 243 and 283 K with helium as the third body. As a consequence of experimental limitations, all experiments were conducted at $P = 2$ Torr. At this pressure, the reaction is in its low-pressure, third-order limiting regime. The dependence on temperature could be expressed as a simple (negative) power of the temperature, with an exponent virtually identical with that found by Burkholder *et al.*[11] using N_2 as third body. Comparison of our data with those of Burkholder *et al.* shows that N_2 is rather more than twice as effective a third body as is He.

Combination of the rate coefficient for the formation of Cl_2O_3 with the measured equilibrium constant at each temperature permitted us to calculate the rate of thermal decomposition of Cl_2O_3 as a function of temperature. The data fitted an Arrhenius expression very closely. Using our estimates for relative efficiencies of He and N_2 as third bodies in the forward reaction of formation of Cl_2O_3, we have suggested an expression for the temperature-dependent rate constant for decomposition of Cl_2O_3 when $M = N_2$ in the low-pressure, second-order, regime. This expression might usefully replace the limited information currently available in data compilations.[24]

The kinetic data for the rates of formation and decomposition of Cl_2O_3 can now be used for reliable extrapolation to stratospheric temperatures and pressures. The data indicate that the oxide can at most be only a minor reservoir for chlorine species. The precursors ClO and OClO only co-exist during limited parts of the diurnal and seasonal cycles, and ClO may be largely consumed in forming the dimer $(ClO)_2$ rather than Cl_2O_3. The thermal decomposition of Cl_2O_3 is rapid, the lifetime being only a few tens of seconds even at the lowest temperatures encountered in the polar stratosphere, so that the reservoir, in as much as it exists at all, is only transitory. Even when the stratosphere is exposed to sunlight, thermal decomposition dominates over photolysis in the loss of Cl_2O_3.

Acknowledgements

The authors wish to record their indebtedness to the contributions to this investigation made by Jason Windsor while he conducted research in Oxford for his Part II project. The authors gratefully acknowledge support for this research from NERC (grant GST/02/0871; formerly SERC grant GR/H/56311), and from the CEC under contracts STEP 0012-C (HALOX), EV5V CT910016 (CHAOS) and PL931392 (CABRIS). T. J. G. wishes to thank NERC for a research training award (GTST/43/ACH/6).

References

1 M. Faraday, *Philos. Trans. R. Soc. London*, 1823, **113**, 189.
2 R. P. Wayne, G. Poulet, P. Biggs, J. P. Burrows, R. A. Cox, P. J. Crutzen, G. D. Hayman, M. E. Jenkin, G. Le Bras, G. K. Moortgat, U. Platt and R. N. Schindler, *Atmos. Environ.*, 1995, **29**, 2675.
3 W. Wongdontri-Stuper, R. K. M. Jayanty, R. Simonaitis and J. Heicklen, *J. Photochem.*, 1979, **10**, 163.
4 M. I. López and J. E. Sicre, *J. Phys. Chem.*, 1990, **94**, 3860.
5 R. L. Mauldin, J. B. Burkholder and A. R. Ravishankara, *J. Phys. Chem.*, 1992, **96**, 2582.
6 R. L. Mauldin, J. B. Burkholder and A. R. Ravishankara, *Int. J. Chem. Kinet.*, 1997, **29**, 139.
7 S. Solomon, *Nature (London)*, 1990, **347**, 347.
8 F. J. Lipscomb, R. G. W. Norrish and B. A. Thrush, *Proc. R. Soc. London Ser. A*, 1955, **233**, 455.
9 G. D. Hayman and R. A. Cox, *Chem. Phys. Lett.*, 1989, **155**, 1.
10 A. D. Parr, R. P. Wayne, G. D. Hayman, M. E. Jenkin and R. A. Cox, *Geophys. Res. Lett.*, 1990, **17**, 2357.
11 J. B. Burkholder, R. L. Mauldin, R. J. Yokelson, S. Solomon and A. R. Ravishankara, *J. Phys. Chem.*, 1993, **97**, 7597.
12 M. H. Harwood, D. M. Rowley, R. A. Fishwater, R. A. Cox and R. L. Jones, *J. Chem. Soc., Faraday Trans.*, 1995, **91**, 3027.
13 S. P. Sander, R. R. Friedl, D. M. Golden, M. J. Kurylo, R. E. Huie, V. L. Orkin, G. K. Moortgat, A. R. Ravishankara, C. E. Kolb, M. J. Molina and B. J. Finlayson-Pitts, *Chemical Kinetics and Photochemical Data for Use in Atmospheric Studies Evaluation Number* 14 (revised Feb. 2003), Publication JPL 02-25, Jet Propulsion Laboratory, California Institute of Technology, Pasadena, CA.
14 R. J. Derby and W. S. Hutchison, *Inorg. Synth.*, 1953, **4**, 152.
15 T. J. Green, M. Islam, C. E. Canosa-Mas, G. Marston and R. P. Wayne, *J. Photochem. Photobiol. A: Chem.*, 2004, **161**, in press.
16 H. Kromminga, J. Orphal, P. Spietz, S. Voigt and J. P. Burrows, *J. Photochem. Photobiol. A: Chem.*, 2003, **157**, 149.
17 G. Herzberg and K. P. Huber, *Constants of Diatomic Molecules*, Van Nostrand Rheinhold, New York, 1978.
18 M. G. K. Pillai and R. F. Curl, *J. Chem. Phys.*, 1962, **37**, 2921.
19 R. R. Friedl, M. Birk, J. J. Oh and E. A. Cohen, *J. Mol. Spectrosc.*, 1995, **170**, 383.
20 W. J. Hehre, 1993, personal communication.
21 J. B. Burkholder, R. J. Yokelson, S. Solomon and A. R. Ravishankara, *J. Geophys. Res.*, 1993, **98**, 22 937.
22 S. Abramowitz and M. W. Chase, *Pure. Appl. Chem.*, 1991, **63**, 1449.
23 J. E. Sicre and C. J. Cobos, *J. Mol. Struct.*, 2003, **620**, 215.
24 R. Atkinson, D. L. Baulch, R. A. Cox, J. N. Crowley and R. F. Hampson, Jr., Summary of Evaluated Kinetic and Photochemical Data for Atmospheric Chemistry, Webversion,December 2002. (URL: http://www.iupac.kinetic.ch.cam.ac.uk/summary/IUPAC-summ_web_latest.pdf).